  DOI 10.1515/HTMP.2011.123

Wear Characteristics of Sintered Cermets

Róbert Bidulský,[1,*] **Jana Bidulská,**[2]
Freddy Arenas[3] **and Marco Actis Grande**[1]

[1] Politecnico di Torino-Alessandria Campus, Alessandria, Italy
[2] Department of Metals Forming, Technical University of Košice, Slovakia
[3] Department of Materials Technology, University Institute of Technology, Venezuela

Abstract. The present paper deals with the tribological behaviour of the boride and carbide hardmetals evaluated by performing comparative dry sliding pin-on-disc experiments using normal contact loads. Analyses of the wear performance results, microstructural evaluation and processing conditions effect indicate that microstructure inhomogenities play an important role in abrasive wear behaviour of cermets. In term of grain size and chemical composition, the addition of VC also play an important role in increasing the wear resistance.

Keywords. Cermets, sliding wear, friction and microstructure.

PACS®(2010). 81.05.Mh, 81.20.Ev, 81.40.-z, 81.40.Pq.

1 Introduction

Powder metallurgy (PM) is a well-established processing route for the production of near-net-shape components of complex geometry. The traditional uniaxial powder consolidation process is still widely employed for the production of PM parts, especially for the automotive industry; in this field the typical components (i.e. gears, cams) face working conditions giving rise to sliding, rolling or abrasion. Therefore the understanding of wear phenomena and characteristics is very important [1–5].

In general, borides are very interesting materials widely used due to their high melting point, wear resistance, chemical inertness and high hardness values [6–12], as well as WC-Co cemented carbides are well known to possess exceptional properties within a wide temperature range.

* **Corresponding author:** Róbert Bidulský, Politecnico di Torino-Alessandria Campus, Viale T. Michel 5, 15121 Alessandria, Italy; E-mail: robert.bidulsky@polito.it.

Received: May 27, 2011. Accepted: June 14, 2011.

Their unique combination of excellent hardness, wear resistance, toughness and strength explains the extensive use in plenty of applications where excellent mechanical properties are required and heavy service conditions where high wear resistance either in abrasive conditions or at elevated temperatures (high speed cutting) are required [6, 7].

Tungsten carbide (WC) possesses metallic character and, thus, high thermal and electrical conductivity combined with excellent hardness and relatively high toughness. Their most important advantage is the chemical compatibility with metals, enabling easy production. Although the superior toughness of the cermets does not require significant further improvement, the presence of a metal limits the applicability at high temperatures owing to softening. Thus, WC remain interesting materials for ceramic composites, especially as sintering additives [8, 9].

In the present study, the tribological behaviour of the sintered cermets was evaluated using dry sliding pin-on-disc experiments.

2 Experimental Materials and Methods

Table 1 shows the chemical composition (mol. %) of the boride-carbide hardmetals. The design has been made based on the commercial grade 90 wt. % WC - 10 wt. % Co, where WC has been partially substituted by other carbides and/or borides.

No.	WB	WC	Co	VC
7	36.5	36.5	27	–
8	36.5	18.25	27	18.25

Table 1. Chemical composition of the investigated materials.

Specimens were obtained using a MTS hydraulic press, applying pressures of 350 MPa. Processing conditions are presented in Table 2. Densities were evaluated using the water displacement method.

No.	Processing conditions
a	1673 K/3600 s, cooling rate of 15 K/s
e	1573 K/7200 s, cooling rate of 15 K/s

Table 2. Processing conditions with data of sintering temperature, time and cooling rate.

Wear tests were carried out by means of a pin-on-disc apparatus. The disc was made of the investigated material. As a counter face, a WC-Co pin was used. The counter-pin was changed after the end of each test, in order to preserve the roundness of its top. All wear tests were performed in air and without any lubricant. The applied loads were 25 N. The rotation speed of the disc was 140 rpm. Prior to testing the surface was polished with abrasive papers in order to determine a medium surface roughness equal (or less) to $0.8 \cdot 10^{-6}$ m, as specified in the ASTM G99-95a. Each test was run for 1000 meters sliding distance and discs were weighed, using a precision scales with a sensitivity of 10^{-5} g to determine the evolution of wear during each test. The surface topography was measurement by Hommel Tester T1000 tangent profilometer.

The metallographic specimens were impregnated with resin under vacuum in order to avoid any pore distortion during polishing. The microstructural characterization was carried out on unetched specimens using an LEICA MPEF4 equipped with an image analyzer and Jeol 7000F.

Mass losses were expressed as material removal during the test. The wear of sintered materials is more complicated than that of wrought steels and depends on some factors related to the sintered microstructures as well as porosity. Hence, the evaluation of the wear resistance is better expressed in terms of wear rate. The wear rate has been calculated using the following equation:

$$W_s = \frac{\Delta m}{\rho \cdot L \cdot F_N}, \tag{1}$$

where:

- W_s is the wear rate (mm^3/Nm),
- Δm is the mass loss of test samples during wear test (kg),
- ρ is the density of test materials (kg/m^3),
- L is total sliding distance (m),
- F_N is the normal force on the pin (N).

3 Results and Discussion

Figure 1 shows the friction coefficient behaviour.

In all cases, the recorded curves in Figure 1 show that the friction coefficient increases rapidly from the start to the 200 metres of sliding and subsequently decreases. After the initial stage, the variations in the curves become smaller and the coefficient of friction reaches a stable (steady state), slightly fluctuating value during the remaining testing time. The friction coefficient in steady state is given in the Table 3, together with mass loss data and some important characteristics for powder metallurgy materials, such as density and total porosity.

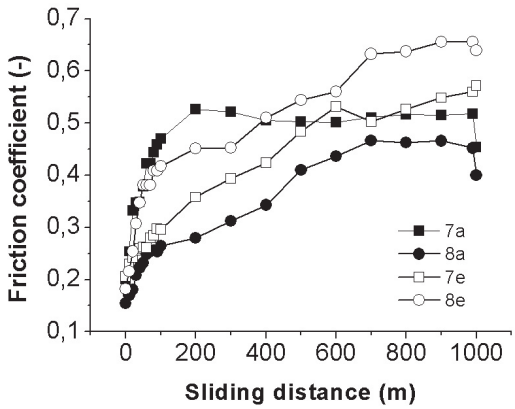

Figure 1. Friction behaviour of sintered cermets.

The friction behaviour of sintered cermets in the first period of wear test can be attributed to a process of polishing, generating a smooth wear track surface, by ploughing away the surface asperities. Surface layer removal and an increase in adhesion due to the increase in clean interfacial areas, as well as increased asperity interactions and wear particle entrapment, lead to a gradual increase in the friction coefficient without and/or up to peak value of friction coefficient. This assumption is very well documented by surface roughness, mainly for 7a material, which shows the clearly observed peak value of friction coefficient, Table 4.

No.	Density ($\cdot 10^6$ g/m^3)	Total Porosity (%)	Steady-state of friction (–)	Mass loss ($\cdot 10^{-3}$ g)
7a	11.71	0.93	0.5087	0.496
8a	10.78	0.57	0.4576	0.540
7e	12.85	0.84	0.5029	0.232
8e	11.39	0.67	0.6452	0.243

Table 3. Material and wear characteristics in investigated sintered cermets.

No.	Perpendicular direction		Parallel direction	
	Ra ($\cdot 10^{-6}$ m)	Rt ($\cdot 10^{-6}$ m)	Ra ($\cdot 10^{-6}$ m)	Rt ($\cdot 10^{-6}$ m)
7a	0.085	2.79	0.10	4.34
8a	0.08	1.31	0.08	1.605
7e	0.04	1.18	0.04	1.595
8e	0.04	1.105	0.06	1.815

Table 4. Surface roughness in perpendicular and parallel direction of studied materials.

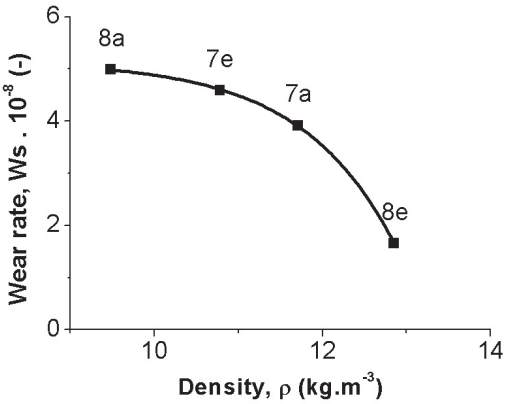

Figure 2. Wear rate of sintered cermets.

As the process proceeds further, the wear track becomes smoother and the friction coefficient achieved on a steady state.

The surface roughness influenced the friction coefficient, mainly in the first period of the run test. The relationship between the wear and the surface topography are supported also by other authors [10–12].

The wear rates are presented Figure 2.

It is very clear show that wear rate exponentially dependence on density value of investigated materials:

$$y = y_0 + A \cdot \exp^{(-x/t)}, \tag{2}$$

where: $A = -3.3 \cdot 10^{-5}$, $y_0 = 5.149$, $t = -1.1108$.

The better explanation of wear rate behaviour of investigated materials may be found in the analysis of the wear tracks and worn surfaces. The wear tracks of the investigated material are presented in Figures 3–6.

The evaluation of SEM structures points out some uniform features. In all cases, the wear processes starts via the plastic deformation of the surface irregularities and/or ploughing away (mechanical polishing) the surface asperities therefore the surface becomes a smooth surface. It is very clear that some "islands" were formed by loose debris from the pin counterphase and also by the product of the adhesion junctions of both sliding surfaces (mainly in the Figures 3 (b), 4 (b), 5 (b) and 6 (b)).

It is well known that the cermets matrix plays an important role in the wear behaviour. Pirso et al. [16] stated that the weakest structural elements in cermets are usually the boundaries between carbide grains (carbide–carbide) or phases (carbide–binder). Therefore, the sliding wear of cermets starts by plastic deformation (abrasion) of the soft ductile Co matrix between WC particles. The wear products from deformed cobalt removal of the binder phase at the surface from between the tungsten carbide grains. This assumption is confirmed by SEM observation. In all worn microstructures present several pits formed by removal of grains by the above described mechanism.

The results is in good agreement with other authors [17–22].

SEM analysis reveals that the main wear mechanism in material 7 (WB-WC-Co) were initial expulsion of surface cobalt binder phase from between the tungsten carbide, followed by deterioration and/or detachment of carbide grains by cracking and/or fracture. These wear behaviour is in agreement with other authors [13–16].

The detailed study of wear tracks of material 8 (WB-WC-Co-VC) reveals that the prevailed war mechanism is abrasive wear. In terms of friction behaviour, VC lowers the friction coefficient in the tribological pair by the formation of a vanadium oxy-carbide [17] and the detail investigation of wear tracks reveal that some abrasive-erosion wear occurred. Klaasen et al. [21, 22] stated that the abrasive-erosion wear resistance of cermets depends primarily on the properties (strength and rigidity) of the carbide phase and then on those of the binder.

Considering the previous statement about exponential dependence of wear rate on density value and results to take from SEM analysis, it is possible to summarize that density (porosity) is a dominant microstructural factor and that the present cavity (voids) influenced the boundaries between carbide grains (carbide–carbide) or phases (carbide–binder) as a possible source of cracks due to the highly stress concentrators. Consequently, microstructure inhomogenities can be play more important role in abrasive wear behaviour of cermets. Moreover, it is well known [15–17, 23–25] that the wear resistance of cemented carbides generally increases as the volume fraction of cobalt decreases and increases dramatically as WC grain size is reduced. More particularly, a considerable improvement in wear performance of cemented carbides is acquired when the WC grain size is reduced towards nanometer.

In terms of nanosize methods, in present time in PM area, are very promising methods are SPD (Severe Plastic Deformation) methods, such as ECAP, ECAP-BP or ECAR [26–30]. Another and proven method for downsizing the final grain size in cemented carbides is grain growth inhibition by adding small amounts of VC during liquid phase sintering.

The present results show that the right way for improving the wear resistance of cermets are to increase its strength-resistance to extraction and adhesive interaction and adding of inhibitors, such as VC, for downsizing the final grain size.

4 Conclusions

The obtained results can be summarized as follows:

1. Microstructure inhomogenities (cavity as a stress concentrators, soft binder phase cracks, the boundaries between

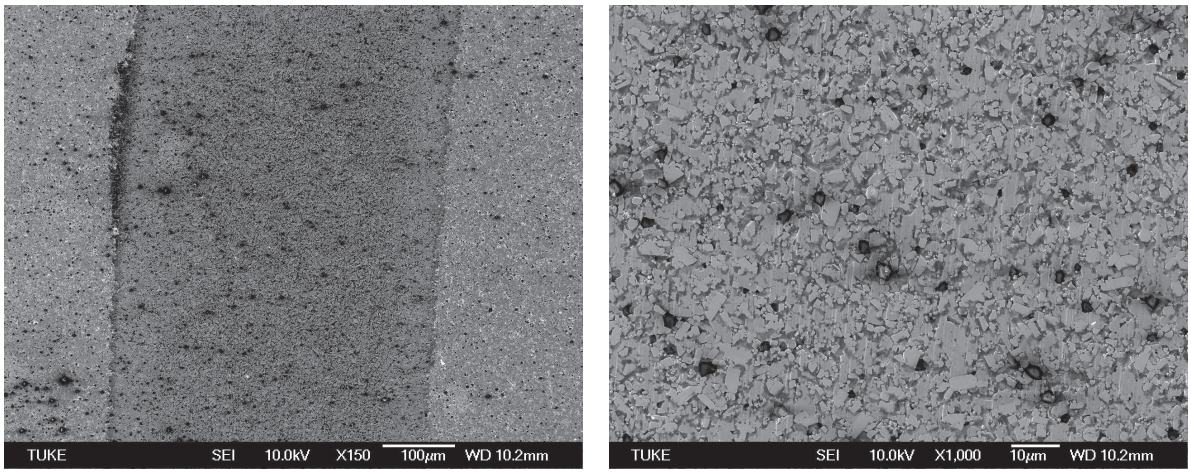

(a) **(b)**

Figure 3. The typical wear tracks for 7a specimen and detail of worn mirostructures.

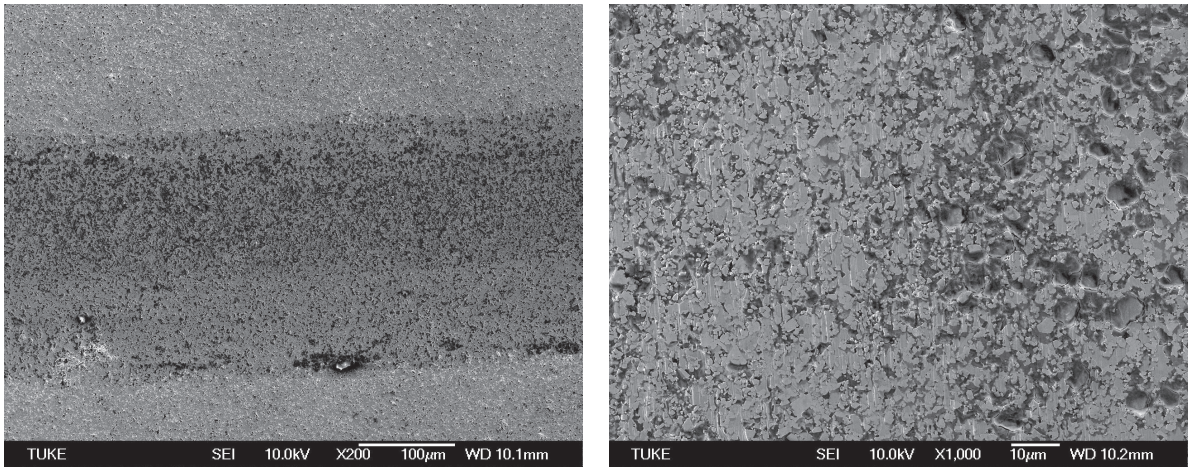

(a) **(b)**

Figure 4. The typical wear tracks for 7e specimen and detail of worn mirostructures.

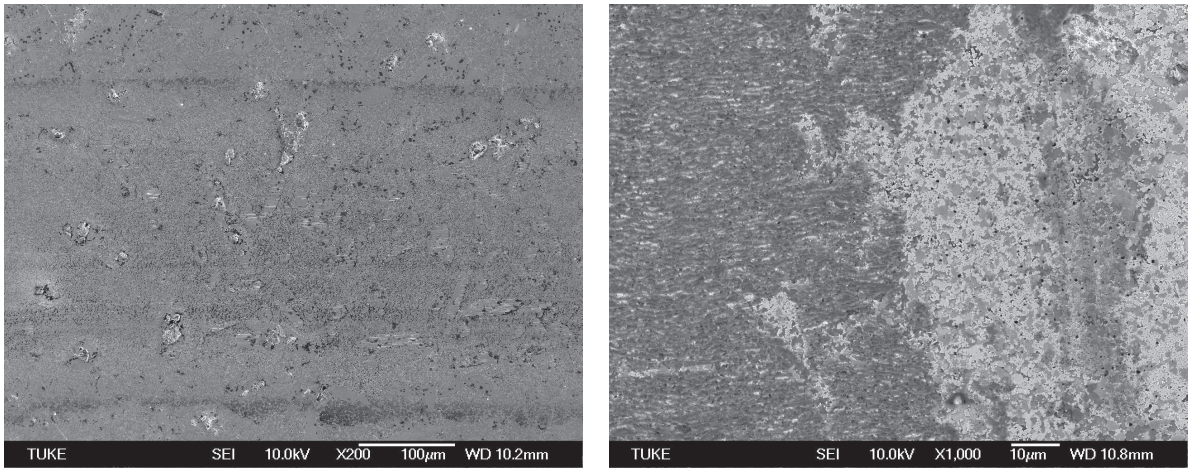

(a) **(b)**

Figure 5. The typical wear tracks for 8a specimen and detail of worn mirostructures.

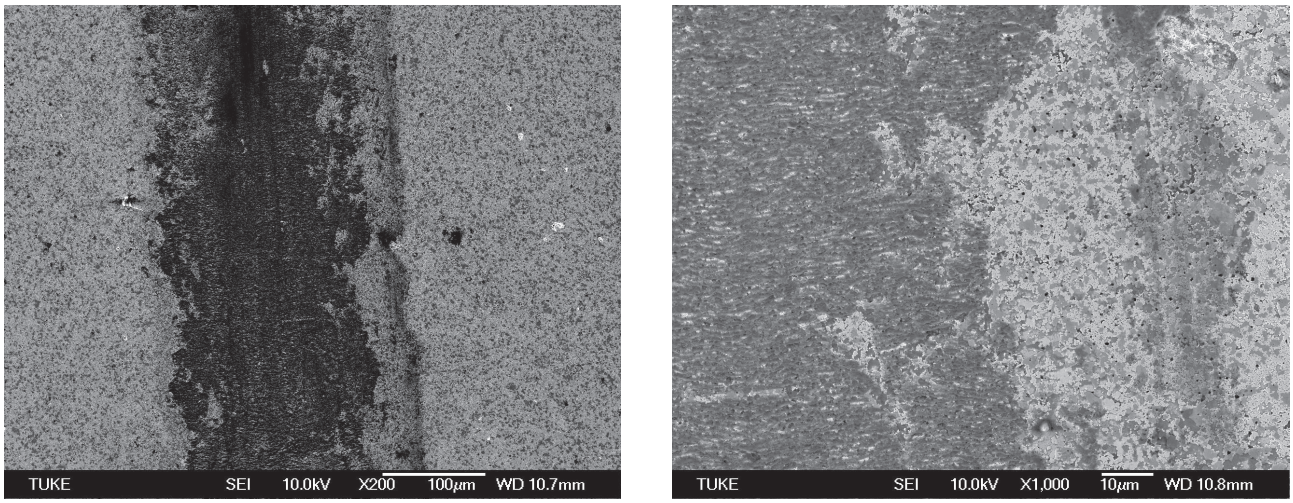

(a) **(b)**

Figure 6. The typical wear tracks for 8e specimen and detail of worn mirostructures.

carbide grains or carbide-binder phases) can be play more important role in abrasive wear behaviour of cermets.

2. In term of grain size and chemical composition, addition of VC play important role in increasing the wear resistance.

Acknowledgments

R. Bidulský thanks the Politecnico di Torino and the Regione Piemonte for co-funding the fellowship.

References

[1] R. Bidulský and M. Actis Grande: *High Temp. Mater. Process.*, **27**, No. 4 (2008), 249–256.

[2] R. Bidulský, M. Actis Grande, J. Bidulská and T. Kvackaj: *Mater. Tehnol.*, **43**, No. 6 (2009), 303–307.

[3] R. Bidulský, M. Actis Grande, J. Bidulská, M. Vlado and T. Kvackaj: *High Temp. Mater. Process.*, **28**, No. 3 (2009), 175–180.

[4] R. Bidulský, M. Actis Grande, A. Zago, Z. Brytan and J. Bidulská: *Arch. Metall. Mater.*, **55**, No. 3 (2010), 623–629.

[5] J. Bidulská, R. Bidulský and M. Actis Grande: *Acta Metall. Slovaca*, **16**, No. 3 (2010), 146–150.

[6] A. Sáez, F. Arenas and E. Vidal: *Int. J. Refract. Met. Hard Mat.*, **21**, No. 1–2 (2003), 13–18.

[7] H. Klaasen, J. Kübarsepp: *Wear*, **256**, (2004), 846–853.

[8] R. Telle and G. Petzow: *Mater. Sci. Eng. A*, **105–106**, No. 1 (1988), 97–104.

[9] P. A. Dearnley, M. Schellewald and K. L. Dahm: *Wear*, **259**, No. 7–12 (2005), 861–869.

[10] E. C. Teague, F. E. Scire and T. V. Vorburger: *Wear*, **83**, No. 1 (1982) 61–73.

[11] K. J. Stout and E. J. Davis: *Wear*, **95**, No. 2 (1984), 111–125.

[12] E. P. Whitenton and P. J. Blau: *Wear*, **124**, No. 3 (1988) 291–309.

[13] M.G. Gee, A. Gant and B. Roebuck: *Wear*, **263**, No. 1–6 (2007), 137–148.

[14] J. Pirso, S. Letunovits and M. Viljus: *Wear*, **257**, No. 3–4 (2004), 257–265.

[15] J. Pirso, M. Viljus and S. Letunovits: *Wear*, **260**, No. 7–8 (2006), 815–824.

[16] K. Bonny, P. De Baets, J. Vleugels, S. Huang, O. Van der Biest and B. Lauwers: *Wear*, **267**, No. 9–10 (2009), 1642–1652.

[17] F. Arenas, C. Rondón and R. Sepúlveda: *J. Mater. Sci. Technol.*, **143–144**, No. 1 (2003), 822–826.

[18] M. Komac and S. Novak: *Int. J. Refract. Met. Hard Mat.*, **4**, (1985), 21–26.

[19] E.T. Jeon, J. Joardar and S. Kang: *Int. J. Refract. Met. Hard Mat.*, **20**, (2002), 207–211.

[20] J. Larsen-Basse: *Wear*, **105**, No. 3 (1985), 247–256.

[21] J. Kübarsepp, H. Klaasen and J. Pirso: *Wear*, **244**, (2001), 229–235.

[22] H. Klaasen and J. Kübarsepp: *Wear*, **256**, (2004), 846–853.

[23] K. Bonny, P. De Baets, J. Vleugels, S. Huang, O. Van der Biest and B. Lauwers: *Wear*, **267**, No. 9–10 (2009), 1642–1652.

[24] F. Arenas, A. Matos, M. Cabezas, C. Di Rauso, C. Grigorescu: *Int. J. Refract. Met. Hard Mat.*, **19**, No. 4–6 (2001), 381–387.

[25] R. Sepúlveda, F. Arenas: *Int. J. Refract. Met. Hard Mat.*, **19**, No. 4–6 (2001), 389–396.

[26] J. Bidulská, R. Kocisko, R. Bidulský and M. Actis Grande: *Acta Metall. Slovaca*, **16**, No. 1 (2010), 4–11.

[27] J. Bidulská, T. Kvackaj, R. Bidulský and M. Actis Grande: *High Temp. Mater. Process.*, **27**, No. 3 (2008), 203–207.

[28] R. Bidulský, J. Bidulská and M. Actis Grande: *High Temp. Mater. Process.*, **28**, No. 5 (2009), 337–342.

[29] A. Kovácová, M. Kvackaj, T. Kvackaj, R. Kocisko and T. Donič: *Acta Metall. Slovaca*, **16**, No. 2 (2010), 91–96.

[30] M. Kvackaj, T. Kvackaj, A. Kovácová, R. Kocisko and J. Bacsó: *Acta Metall. Slovaca*, **16**, No. 2 (2010), 84–90.